XLIII CILAMCE
21-25, November, 2022
FOZ DO IGUAÇU - PR - BRAZIL

Numerical study on fiber-reinforced concrete using finite element method

Luiza Maria da Silva Santos[1], Lia Beatriz G. Furtado[1], Marcelo S. Medeiros Jr[1], Joaquim E. Motta[1]

[1]*Dept. of Structural Engineering and Civil Construction, Federal University of Ceará*
Campus Universitário do Pici, 60455-760, Ceará, Brazil
luizamss@alu.ufc.br, liagomes@alu.ufc.br, marcelomedeiros@ufc.br, jemota@fortalnet.com.br

Abstract. Different techniques have been recently developed to increase the tensile and shear strength of reinforced concrete elements in addition to improving their durability. Fiber-reinforced concrete (FRC) has been the target of many studies, since it presents a higher tensile strength and toughness when compared to regular concrete, thus reducing crack growth, and increasing the concrete's durability. In this study, a finite element analysis was carried out to simulate the behavior of FRC and normal concrete beams under four-point loading conditions. A parametric study was set to evaluate the influence of the the steel fibers concentration and stirrups ratios. The ABAQUS Concrete Damaged Plasticity (CDP) model was used to describe the material's constitutive behavior. The ultimate bending capacities of the beams simulated were compared against the models proposed in the ABNT NBR 16935:2021. Experimental results from the literature were compared to the results were found to be in accordance with the finite element simulations and with the ultimate flexural capacity analytical solution proposed by the NBR standard. The study showed that the finite element simulation method using the CDP model predicts load-displacement curves slightly more stiffer than the experimental results nevertheless in good agreement with the analytical models proposed by NBR 16935:2021.

Keywords: Fiber-reinforced concrete, Flexural loading capacity, Finite element method, Concrete Damaged Plasticity

1 Introduction

Concrete is a naturally brittle material. Over the years, several technologies were developed to increase its ductility and improve its tensile strength in order to overcome its brittle behavior. In the 60's, fiber-reinforced concrete (FRC) became the technique of choice to mitigate these issues. Since then, multiple studies were carried out in order to study the flexural behaviour and shear behaviour of steel fiber-reinforced concrete beams.

Adding steel fibers to concrete provides residual strength after cracking, given that the fibers bridge across the cracked matrix, transferring tensile stress across the cracked section [1]. Steel fibers are generally employed as reinforcement due to its high elasticity modulus and its good adherence to the concrete. Moreover, it can also work as the primary reinforcement or in combination with conventional rebars [2]. Many parameters influence the response of the FRC on the post-cracking behavior such as shape and geometry of the steel fiber, the concrete matrix, fiber content and distribution of the fibers [3].

Fibers have a strong influence on the workability of the concrete during its the fresh state, especially at high fiber contents. This characteristic limits the amount of fibers added to the mixture to a maximum of 3%.

Given the qualitative aspects of fiber incorporation, this study seeks to assess the ultimate flexural strength of FRC beams compared to ordinary concrete using the formulation presented by the ABNT NBR 16935 standard [4] and analysis through the finite element method.

The numerical model adopted in this study accounted for the influence of the volume fraction of steel fibers and different stirrup ratios. The mechanical responses of the simulated beams were validated against the experimental tests carried out by Lim and Oh [5].

2 Concrete Damage Plasticity model

The Concrete Damage Plasticity model in ABAQUS allows concrete and other quasi-brittle materials to be modeled as homogeneous materials predicting its behavior within the framework of a non-associated plasticity coupled to a damage evolution law. For FRC, it is assumed that fibers are uniformly distributed in the matrix forming a continuum media. Under tensile stress, the regular concrete is assumed to have a linear elastic response until the tensile strength,σ_{t0}, is reached. This point corresponds to the coalescence of micro cracks in the material and from there on, the constitutive behavior is represented by a softening stress-strain response [6]. However due to the added ductility from the metal fibers, the constitutive behavior under tensile stress was assumed to follow the behavior seen in Fig 1a.

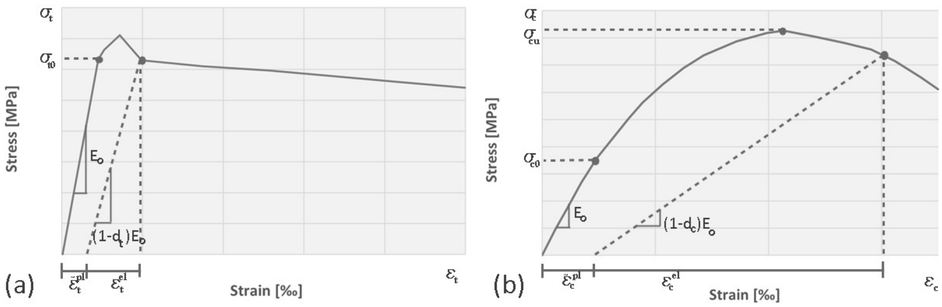

Figure 1. Uniaxial stress–strain curve for 1% fiber concrete with damage in tension (a) and compression (b)

The CDP model also assumes that the failure in compressive crushing of concrete follows the constitutive laws shown in Figure 1b. This model is able to address the major characteristics of the typical response of concrete under a multiaxial state of stress.

Meanwhile, the response under compression is linear up to the initial yield value σ_{c0}. Then, the plastic regime starts and the stress-strain relationship is characterized by stress hardening until the ultimate compressive strength, σ_{cu}, is reached, followed by strain softening [6].

In addition to stress-strain curves, the CDP model requires five plasticity parameters to define the yield surface in the multiaxial state. These parameters are, dilatation angle, ψ, eccentricity, *e*, relationship between the compressive strength of biaxial and uniaxial concrete, σ_{cb0}/σ_{c0}, form factor, K_c, and viscosity, μ. The process of determining the parameters must be done meticulously since the results provided using the CDP model are sensitive to this choice.

3 Ultimate load capacity calculation method

The tensile response of the FRC can present an increase of the load capacity after the first crack, called a strain hardening or the composite can present a strain softening behavior, by decreasing the load capacity after the first crack. To determine the FRC residual post-cracking tensile strength, a three-point bending test is recommended by the ABNT NBR 16940 [7], 2021 standard. This test provides a curve of applied force (F) versus the opening of the notch at the bottom of the beam, called Crack Mouth Opening Displacement (CMOD). The response of the FRC in tension is then expressed in terms of residual flexural tensile strength $f_{R,j}(j = 1, 2, 3, 4)$ versus $CMOD_j(CMOD_1 = 0.5mm, CMOD_2 = 1.5mm, CMOD_3 = 2.5mm, CMOD_4 = 3.5mm)$.

With that information, it is possible to determine the direct tensile strength of FRC. According to ABNT NBR 16935 [4] standard, the process to determine the FRC compressive strength is the same as in conventional concrete. Meanwhile, the tensile strength, which is not considered in conventional concrete, can be determined through two different hypotheses of constitutive laws: the rigid-plastic model and the linear model. Both models present post-cracking behavior of hardening and softening, as shown in Figure 2.

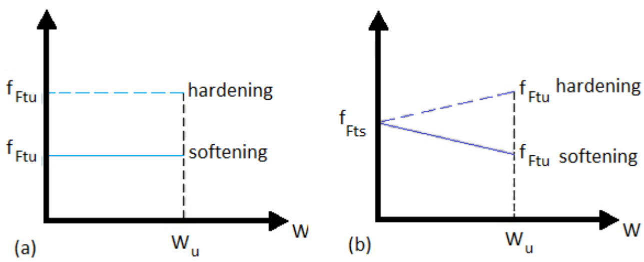

Figure 2. Simplified constitutive laws (a) rigid-plastic model and (b) linear model [7]

3.1 Rigid-plastic model

In the rigid-plastic model, there is an assumption that the post-crack residual tensile stress is uniformly distributed throughout the cross section and the compressive stress is concentrated in the upper fiber of the section. The value of ultimate residual tensile strength f_{Ftu} is sufficient to define the rigid-plastic model and, assuming the maximum crack opening accepted in structural design w_u as $CMOD_3$, can be determined as shown in Figure 3.

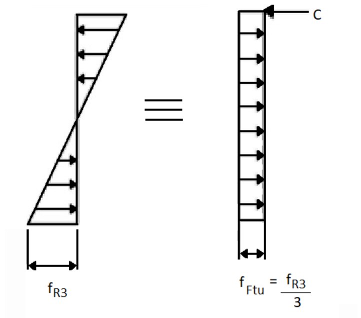

Figure 3. Rotational equilibrium for the rigid plastic model [4]

The characteristic bending moment due to the contribution of the fibers, M_{Uk}, acting on the section is calculated by:

$$M_{Uk} = \frac{f_{R3}bh^2}{6} = \frac{f_{Ftu}bh^2}{2} \tag{1}$$

The total moment capacity calculated by the rigid-plastic model, $M_{rd(RP)}$, is defined by the sum of the design bending moment due to the contribution of the fibers, M_{Ud}, and the bending moment for conventional concrete, M_{d1}, calculated according to the ABNT NBR 6118 - Design of concrete structures — Procedure [8] standard, as illustrated in figure 4.

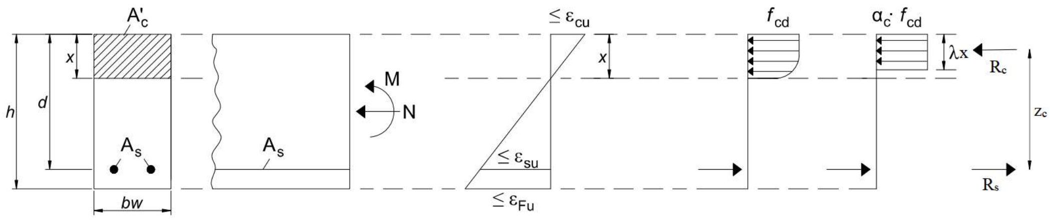

Figure 4. Stress block diagram for normal concrete beams [4]

The calculation equations and symbols are described accordingly in the NBR standard 6118 [8]. The equations are expressed by Equations (2), (3) and (4):

$$R_c = \alpha_c \cdot f_{cd} \cdot \lambda \cdot x \cdot b \tag{2}$$

$$R_s = f_{yd} \cdot A_s \tag{3}$$

$$M_{d1} = \alpha_c \cdot f_{cd} \cdot \lambda \cdot x \cdot b(d - \frac{\lambda}{2}x) \tag{4}$$

3.2 Linear model

The linear model requires the identification of two reference values: serviceability residual strength f_{Fts} and ultimate residual strength f_{Ftu}, which are defined through residual values of flexural strength by using the following expressions:

$$f_{Fts} = 0,45 f_{R3} \tag{5}$$

$$f_{Ftuk} = f_{Fts} - \frac{w_u}{CMOD_3}(f_{Fts} - 0,5f_{R3} + 0,2f_{R1}) \geq 0 \tag{6}$$

For the linear model, the ULS diagram is shown in Figure 5. In this case, fibers are taken into account, so the equilibrium equations have three resistant values, the concrete one R_c, given by Equation (2), the steel one R_s, given by Equation (3), and fiber reinforcement one R_f, given by Equation (7).

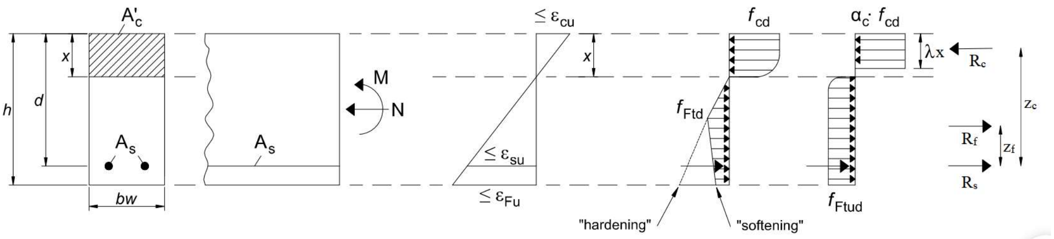

Figure 5. Stress block diagram for fiber-reinforced concrete beams [4]

$$R_f = f_{Ftud} \cdot (h - x) \cdot b \tag{7}$$

The moment acting in the section calculated by the linear model is defined by:

$$M_{rd(L)} = f_{Ftud} \cdot (h - x) \cdot b((\frac{h-2}{2}) - a) - \alpha_c \cdot f_{cd} \cdot \lambda \cdot x \cdot b(d - \frac{\lambda}{2} \cdot x) \tag{8}$$

4 Experimental four-point bending test [5]

The data used in this study was based on the experimental work by Lim and Oh [5]. Using the FE modeling software ABAQUS, three-dimensional models were created to predict the behavior of FRC and regular concrete beams under a four-point bending test. Various simulations were carried out to test beams with rectangular cross sections of 100 x 180 mm and a span length of 1300 mm.

The main goal of the tests is to verify the influence of different percentages of steel fibers in the matrix of concrete and shear reinforcement ratio in the ultimate load reached. Beams were tested with steel fiber contents of 0%, 1% and 2% and containing 0% to 50% of the stirrups required to resist the shear forces. Lim and Oh [5] determined the shear reinforcement required for the experimental beams tested. For a 50% ratio, 6 mm diameter stirrups were allocated with a 80 mm spacing along a shear span length of 400 mm, as shown in Figure 6. The identification of the beams was established according to the stirrup ratio (S0 and S50) and fiber content (V0, V1 and V2).

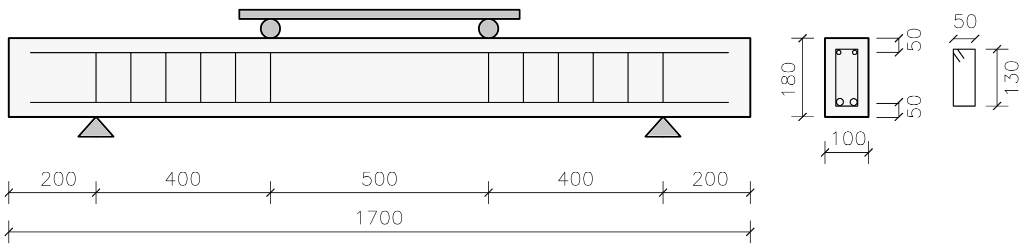

Figure 6. Geometry of FRC and regular concrete beams tested by Lim and Oh [5] with 50% of the shear reinforcement required. (Dimensions in mm)

The longitudinal reinforcement is composed by two 16 mm tension bars and two 10 mm compression bars with yield strength of 420 MPa. Meanwhile, the yield strength of the shear reinforcement is 359 MPa. Both types of steel present an elasticity modulus of 200 GPa and an elastoplastic behavior.

4.1 Material characterization

The steel fibers incorporated into the concrete matrix have a 0.7 mm diameter, 42 mm length, ultimate strength of 1784 MPa, and an aspect ratio of 60. Based in the data presented by Lim and Oh (1999) [5], Matos (2021) [9] determined the uniaxial compressive and tensile strengths of concrete, as well as the modulus of elasticity for different fiber ratios, as shown in Table 1.

Table 1. Mechanical properties of concrete beams tested by Lim and Oh (1999) [5] and Matos (2021) [9]

Fiber ratio (%)	Concrete compressive strength (MPa)	Concrete tensile strength (MPa)	Young's Modulus (MPa)
0	34	3.14	32329.4
1	40.9	3.56	34092.3
2	47.24	3.92	35881.25

Matos (2021) [9] also presents normal concrete and FRC concrete residual strengths $f_{R,1}$ and $f_{R,3}$, used to determine uniaxial tensile strengths f_{Fts} and f_{Ftu}, as shown in Table 2.

Table 2. Residual strength of concrete determined by Matos (2021) [9] based in the experiments done by Lim and Oh (1999) [5]

Fiber ratio (%)	$f_{R,1}(MPa)$	$f_{R,3}(MPa)$
0	2.16	2.41
1	6.92	8.18
2	11.54	13.81

4.2 Finite element modeling

The beams were analyzed using 8-node brick elements (C3D8I) to model the concrete and 2-node linear 3D truss elements (T3D2) to model the reinforcements bars. The reinforcements bars are embedded in the concrete with a perfect bond. The mesh size set for beam parts is 20 mm and the mesh size set for steel parts is 25 mm.

The load was applied as an prescribed displacement at a reference point coupled to the two loading locations to simulate a displacement-controlled mode (see Figure 7). The load-displacement graph is built from the reaction force at the reference point coupled to the nodes that compose the boundary condition of the support and the displacement in a midspan node of the beam.

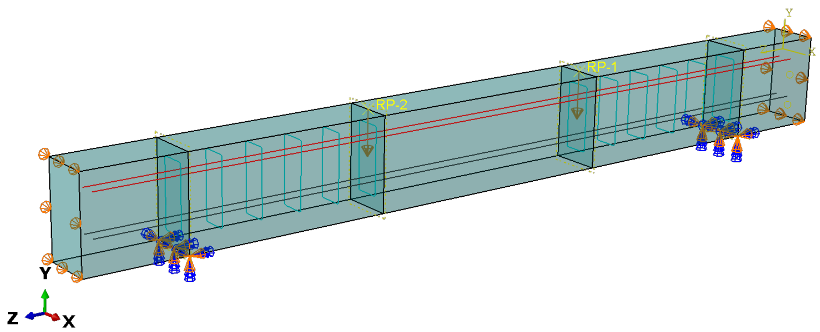

Figure 7. Finite element model in ABAQUS

The plasticity parameters for CDP modeling used in the research were chosen carefully and are summarized in Table 3.

Table 3. Concrete Damaged Plasticity (CDP) parameters

Parameter	Value
ψ	37º
e	0
σ_{cb0}/σ_{c0}	1.16
K_c	1
μ	0.0001

5 Results and analysis

The comparison between the load versus midspan deflection curves for numerical and experimental data for beams with and without stirrups are shown in Figures 8 and 9.

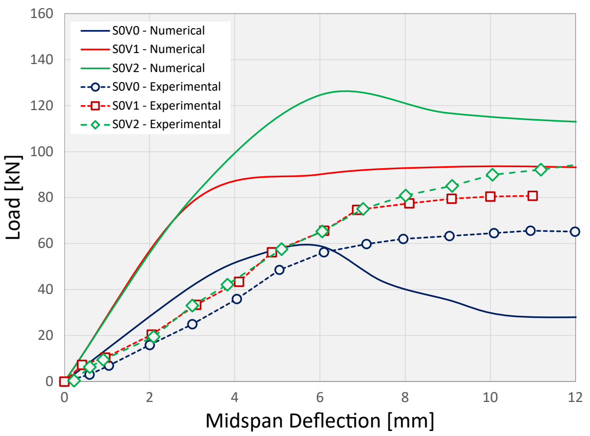

Figure 8. Load-deflection curves for the beams without stirrups

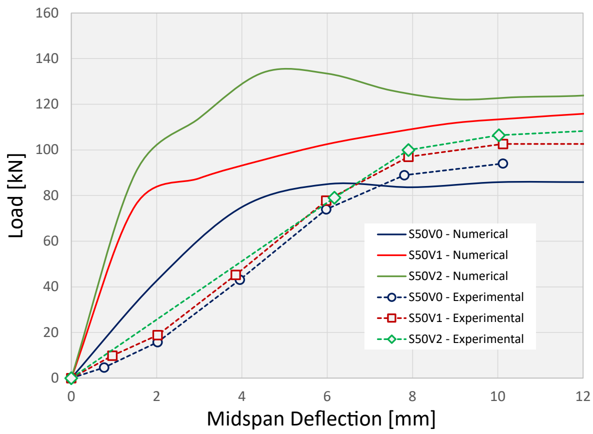

Figure 9. Load-deflection curves for the beams with 50% of the calculated stirrups

The numerical models present results consistent with the experimental tests, beginning with a linear curve until reaching the first crack, then showing nonlinear load-deflection characteristics. However, for all the cases, the numerical results present greater stiffness than the experimental results. This fact can be due to the type of finite element chosen, the definition of the material and the fact that the self-weight of the elements modelled were not considered. The self-weight of the beams can lead to the appearance of small stresses in the element, reducing the stiffness of the beam, decreasing its strength and ductility.

The increase in the percentage of fibers in beams with no stirrups leads to higher ultimate loads and greater ductility. The same phenomenon occurs for beams with stirrups, however to a lesser extent. Note that the addition of shear reinforcement has a similar effect in the load-displacement curves as the incorporation of fibers. It can be concluded that the amount of shear reinforcement necessary can be reduced with the addition of steel fibers.

The crack pattern for each FE beam at the same load stage is shown in Figures 10 and 11.

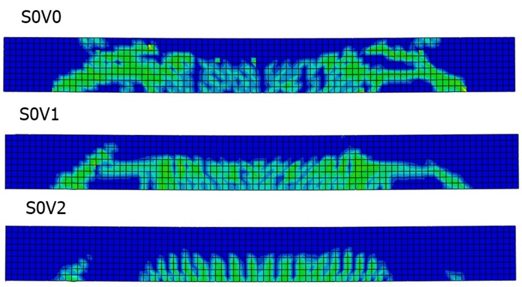

Figure 10. FE prediction of concrete cracks in beams without stirrups

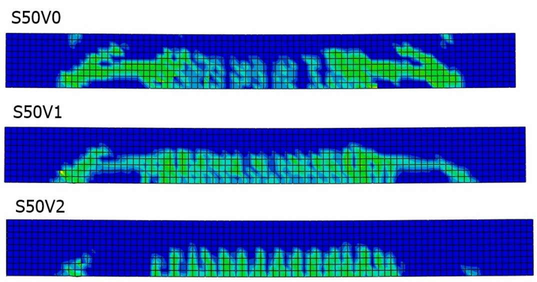

Figure 11. FE prediction of concrete cracks in beams with 50% of the calculated stirrups

The formation of cracks can take place at the supports of the beams due to the stress concentration, however the cracks are mainly distributed in the midspan of the elements. It can be noticed that for beams without fibers, diagonal cracks develop in the beam, potentially leading to failure. As the proportion of steel fibers increases, the crack formation happens in a lower degree. The incorporation of the shear reinforcement has a similar effect, also leading to slightly smaller cracks.

The results of the finite element modeling are compared with the experimental responses and the predictions according to NBR 16935 (2021) [4], as summarized in Table 4. It can be concluded that there is an increase in the bearing capacity of the beams with the increase in the amount of fibers incorporated into the concrete and the addition of stirrups. This behavior is reflected both in numerical and experimental results.

As for the predictions according to NBR 16935 (2021) [4], the results for the rigid-plastic model and linear model are very similar. However, the linear model presents more conservative responses, resulting in a smaller

Table 4. Experimental predictions according to NBR 16935 (2021) [4] and numerical responses for ultimate bending moment

Fiber ratio (%)	$M_{u,exp0\%}$ $(kN.m)$	$M_{u,exp50\%}$ $(kN.m)$	$M_{rd(RP)}$ $(kN.m)$	$M_{rd(L)}$ $(kN.m)$	$M_{u,num0\%}$ $(kN.m)$	$M_{u,num50\%}$ $(kN.m)$
0	13.11	18.81	14.73	14.15	11.78	17.71
1	16.15	21.3	16.81	14.82	18.66	23.71
2	20.55	23.03	18.84	15.39	24.91	26.78

load capacity than the result given by the rigid-plastic model. As expected, the predictions present a factor of safety when compared to Lim and Oh (1999) [5] responses to reduce the risk of failure in the process of beams design.

6 Conclusions

In this study, the behavior of structural FRC and regular concrete beams in four-point bending tests was investigated through the FE method using the ABAQUS CDP model. The load-deflection curves presented by the FE model are slightly higher than the experimental results, due to the CDP model sensitivity to the parameters to be determined. Despite that, the numerical model is able to capture well the FRC behavior before and after cracking.

The numerical model also manages to simulate crack growth direction, as well as the increase in the ultimate strength that occurs with increasing fiber content. The results have shown that the addition of steel fibers to the concrete matrix increases its ultimate strength, ductility and the crack formation. It also can be concluded that the incorporation of fiber reinforcement may allow the amount of required stirrups in a beam to be decreased and, with that information, a balance between the fiber ratio and the amount of stirrups can be sought to achieve higher performance results.

The verification of the bearing capacity of the beams following the recommendations described in the NBR 16935 (2021) [4] presented results with a safety factor. In general, the FE model developed in this study was able to generate good results, showing that numerical studies are an essential tool to contribute on the design of structural elements reinforced with steel fibers.

Authorship statement. The authors hereby confirm that they are the sole liable persons responsible for the authorship of this work, and that all material that has been herein included as part of the present paper is either the property (and authorship) of the authors, or has the permission of the owners to be included here.

References

[1] Bentur, A., Mindess, S. *Fibre Reinforced Cementitious Composites*. Modern Concrete Technology Series, Abingdon, 2007.

[2] Trindade, Y. T. *Numerical modeling of the post-cracking behavior of SFRC and its application on design of beams according to fib Model Code 2010*. Dissertação (Mestrado) - Escola Politécnica da Universidade de São Paulo. Departamento de Engenharia de Estruturas e Geotécnica, São Paulo, 2018. 171 p.

[3] Mehta, P.; Monteiro, P. *Concrete: Microstructure, Properties, and Materials*. McGraw Hill Professional, 2013.

[4] Associação Brasileira de Normas Técnicas. *ABNT NBR 16935: Projeto de estruturas de concreto reforçado com fibras - Procedimento*. 1. ed, Rio de Janeiro, 2021a.

[5] Lim, D. H.; Oh, B. H. Experimental and theoretical investigation on the shear of steel fibre reinforced concrete beams. *Engineering structures, Elsevier*, vol. 21, n. 10, pp. 937–944, 1999.

[6] Online Documentation Simulia. *ABAQUS 6.13 User Manual*. Dassault Systems, 2011.

[7] Associação Brasileira de Normas Técnicas. *ABNT NBR 16940: Concreto reforçado com fibras - Determinação de resistências à tração na flexão (limite de proporcionalidade e resistências residuais) - Método de ensaio*. 1. ed, Rio de Janeiro, 2021b.

[8] Associação Brasileira de Normas Técnicas. *ABNT NBR 6118: Projeto de estruturas de concreto – Procedimento*. 3. ed, Rio de Janeiro, 2014.

[9] Matos, C. C. D. *Análise Numérica de Vigas em Concreto Reforçado com Fibras de Aço Via Método dos Elementos Finitos*. Dissertação (Mestrado) - Universidade Federal do Rio Grande do Sul. Escola de Engenharia. Programa de Pós-Graduação em Engenharia Civil, Porto Alegre, 2021. 181 p.